Available online at www.sciencedirect.com
SCIENCE DIRECT
Journal of Photochemistry and Photobiology A: Chemistry 181 (2006) 378–384
Journal of Photochemistry and Photobiology A:Chemistry
www.elsevier.com/locate/jphotochem

Effects of interaction with CTAB micelles on photophysical characteristics of *meso*-tetrakis(sulfonatophenyl) porphyrin

P.J. Gonçalves [a,*], L.P.F. Aggarwal [a], C.A. Marquezin [a], A.S. Ito [a], L. De Boni [b], N.M. Barbosa Neto [c], J.J. Rodrigues Jr. [d], S.C. Zílio [b], I.E. Borissevitch [a]

[a] *Departamento de Física e Matemática, FFCLRP—USP, Brazil*
[b] *Instituto de Física de São Carlos—USP, Brazil*
[c] *Instituto de Física, Universidade Federal de Uberlândia—UFU, Brazil*
[d] *Universidade Federal do Vale do São Francisco—UNIVASF, Brazil*

Received 14 September 2005; received in revised form 16 December 2005; accepted 19 December 2005
Available online 25 January 2006

Abstract

The whole set of photophysical characteristics of the metal-free water-soluble *meso*-tetrakis(*p*-sulfonatophenyl) porphyrin ($TPPS_4$) in its protonated and nonprotonated states in homogeneous aqueous solutions and in the presence of cationic cetyltrimethylammonium bromide micelles (CTAB) was investigated with nonlinear optical Z-scan technique, UV–vis absorption and fluorescence spectroscopies, time-resolved fluorescence and flash-photolysis. The characteristics were: the cross-sections of the ground (σ_0) and the excited singlet (σ_S) and triplet (σ_T) states; the rate constants of intersystem-crossing (k_{isc}), internal conversion (k_{ic}) and radiative one (k_r); the quantum yields (Φ_{fl} and Φ_T) and lifetimes (τ_S and τ_T) of singlet and triplet states and quantum yield of internal conversion (Φ_{ic}). The study was realized at pH 7.0 and 4.0, where $TPPS_4$ in homogeneous solutions is nonprotonated and biprotonated, respectively. It was observed that, in spite of the fact that protonation changes all these characteristics, their values for $TPPS_4$ bound with CTAB micelles were at both pH close to those of nonprotonated porphyrin in the solution. It is due to the fact that binding with CTAB shifts the p*K* of $TPPS_4$ from 5.0 in homogeneous solution to 2.5 in the micellar one and the bound porphyrin appears in nonprotonated state at both pH used. We can conclude also that the change of the quality of the environment from homogeneous aqueous solution to the micellar one affects weakly the $TPPS_4$ photophysical characteristics when it is not protonated.

Keywords: $TPPS_4$ porphyrin; Photophysical characteristics; CTAB micelles; Fast optical limiters and switches; Photodynamic therapy

1. Introduction

Application of porphyrins and porphyrin-like compounds for photonics devices such as optical limiters and switches has increased significantly over the last decade due to interesting properties of natural and synthetic porphyrins and their derivatives, which possess nonlinear optical absorption and refraction [1–3]. Besides this the interest to study of porphyrin photophysical characteristics is stimulated by their medical applications, especially due to their efficacy in photodynamic therapy (PDT) of cancer [4,5], psoriasis, atheromatous plaque, viral and bacterial infections including HIV [6,7] and blood substitutes [8]. Among them the synthetic water-soluble, thermally and photochemically stable *meso*-tetrakis(*p*-sulfonatofenyl) porphyrin ($TPPS_4$) is studied and used in clinical experiments as a promising sensitizer for PDT [9,10]. Besides this $TPPS_4$ possesses nonlinear optical absorption [11,12], which makes it promising for application in photonic devices.

The porphyrin efficacy in photonic devices and PDT depends on its photophysical characteristics, such as lifetimes and quantum yields of the excited (singlet and triplet) states [1,2,13], which in turn depend on the environmental characteristics: pH, ionic strength, interaction with other molecules, etc. To apply these materials in photonics and medicine in the most effective way it is necessary to know the behavior of all their photophysical characteristics in the function of external conditions. It has already been demonstrated that linear optical characteristics of $TPPS_4$, such as absorption and fluorescence spectra and

* Corresponding author. Present address: DFM, FFCLRP, Universidade de São Paulo, Av Bandeirantes 3900, Vila Monte Alegre, CEP 14040-901, Ribeirão Preto, SP, Brazil. Tel.: +55 16 3602 3862; fax: +55 16 3633 9949.
E-mail addresses: pablo@dfm.ffclrp.usp.br, pablaojg@yahoo.com.br (P.J. Gonçalves).

1010-6030/$ – see front matter © 2006 Elsevier B.V. All rights reserved.
doi:10.1016/j.jphotochem.2005.12.023

fluorescence and triplet state lifetimes along with its nonlinear optical absorption are affected by its interaction with bovine serum albumin and surfactants [11,14–16]. From this point of view, the study of the effects of the $TPPS_4$ interaction with natural or synthetic microorganized system, such as cell membranes, synthetic and biopolymers, micelles, etc., on these characteristics is of a special interest. Generally, the initial step in this study consists in the use of simple microorganized systems, micelles, for example, which can simulate the biological environment and are frequently used as simplified membrane models [17]. On the other hand, this study could supply important information for porphyrin applications in optical devices.

The present work reports on the study of photophysical characteristics of $TPPS_4$ in its biprotonated and nonprotonated states in the presence of cetyltrimethylammonium bromide (CTAB) micelles. The cross-sections of the ground and the excited singlet and triplet states, the rate constants of intersystem-crossing, internal conversion and radiative one, the quantum yields and lifetimes of singlet and triplet states and quantum yield of internal conversion in homogeneous aqueous solutions were compared with those in micelles. In spite of the fact that some of these characteristics have already been measured formerly [18–22] we believe that to apply these materials in photonics and medicine in the most effective way it is necessary to know the behaviour of the whole set of its photophysical characteristics as the function of external conditions.

The nonlinear optical characteristics obtained with Z-scan technique were complemented by the linear ones obtained with UV–vis absorption and fluorescence spectroscopies and time-resolved fluorescence. The results were analyzed and explained by a nonperturbative treatment based on a five-level Jablonsky energy diagram.

2. Materials and methods

The $TPPS_4$ was purchased from Porphyrin Products Inc. and dissolved in Milli-Q quality water. The concentration was monitored spectrophotometrically and pH changes were achieved by the addition of appropriate amounts of HCl or NaOH stock solutions. The surfactant CTAB was obtained from Sigma Co. and used as purchased, always in concentration 4.8 mM, which is higher than critical micellar concentration CMC = 1.0 mM. The experiments were performed at pH 7.0 and 4.0 in Milli-Q quality water at room temperature.

The UV–vis spectra were monitored with a Beckman DU 640 spectrophotometer. The fluorescence spectra were monitored with a Hitachi FL 4500 fluorimeter. Time-resolved experiments were performed using an apparatus based on the time-correlated single photon counting method. The excitation source was a titanium–sapphire laser (Tsunami 3950–Spectra Physics), pumped by the second harmonic of a diode-pumped Nd:YVO_4 laser (Millenia–Spectra Physics) and the frequency doubled to 465 nm in a LBO crystal (GWN-23PL–Spectra Physics).

The triplet state lifetime was monitored with the flash-photolysis technique and was performed in a standard quartz 1 cm cuvette. The $TPPS_4$ excited states were produced by short light pulses (10 ns) of the third harmonic (355 nm) of Nd:YAG laser SL400 Spectron Laser System. The decay profiles of the triplet state absorption were monitored at $\lambda = 470$ nm using a standard detection system. To exclude triplet quenching by molecular oxygen, the samples were usually deoxygenated by bubbling nitrogen through the solution during 30 min and for comparison some of them were deoxygenated with a vacuum pump.

The photophysical parameters of excited states (excited states cross-sections, intersystem crossing rate constants and triplet quantum yield) were obtained by measuring the nonlinear absorption with the open aperture Z-scan technique [23,24]. The Z-scan technique consists basically in monitoring of changes in the light transmittance of a sample when it passes through the focal plane of a tightly focused laser beam. The validity and efficiency of this technique to study excited state parameters of complex conjugated molecules has already been demonstrated [11,12,25,26]. The open aperture configuration collects all the transmitted energy. So, it is sensitive only to the nonlinear absorption and avoid other nonlinear effects, such as thermal lensing, self-focusing and stimulated Raman scattering [27].

In our Z-scan measurements we used a double frequency, *Q*-switched and mode-locked Nd:YAG laser as the pumping source. It produced 70 ps pulses at 532 nm, in pulse trains containing 20 pulses separated by 13 ns intervals. Two regimes of Z-scan were applied: using the single pulse from the *Q*-switch envelope and using the technique called pulse train Z-scan (PTZ-scan), based on application of the complete set of pulses of the *Q*-switch envelope to the sample [28].

Briefly, the PTZ-scan method works as follows: to obtain a reference a pulse train is acquired when the sample position is far from the focal plane, where no nonlinear effect is observed, and every pulse of this train is memorized as the reference one. Subsequently, the sample is moved along the optical axis of the laser beam through the focal plane and various pulse trains affect it during this movement. The amplitudes of every pulse in these trains are compared with the corresponding pulse in the reference one. The analysis of whole pulse set produces the Z-scan signature of the sample. This method allows to map the absorptive nonlinearity along the *Q*-switch envelope and to determine its cumulative contributions. It is possible as the pulses in the train are separated by a time interval, which, on the one hand, is longer than the lifetime of the first singlet excited state (fluorescence lifetime, τ_{fl}) and, on the other hand, is much shorter than the lifetime of the first triplet state of the molecule. This means that the pulse sequence in the train populates the triplet state of the molecule and this population increases with the irradiance of the sample. So the pulse-train method is convenient to determine the triplet state absorption cross-section and the intersystem crossing characteristic time.

The single pulse Z-scan technique is convenient to determine the excited singlet absorption cross-section, since in this case the pulse duration is much shorter than the fluorescence lifetime and during the pulse just first excited singlet state is populated. In this case the population of this state varied due to the changes in the sample irradiance at its displacement across the focal plane via the focus (see the next section for the more detailed explanation). A single 70 ps pulse was extracted from the *Q*-switch envelope

with the help of a Pockels cell sandwiched between two crossed polarizers.

For both regimes, the beam was focused onto the quartz cuvette with $f = 12$ cm lens, resulting in a 40 μm spot in the focal plane. We used a 10 Hz repetition rate to avoid accumulative thermal nonlinearities. The cross-section value was provided by the saturation behavior of several Z-scan curves at different pulse irradiances.

The data reported in this work were the average of three independent experiments.

3. Results and discussion

Due to the presence of nitrogen atoms in its structure, $TPPS_4$ can exist in homogeneous aqueous solutions in various protonation states. The pK values of its first and second protonations (pK_1 and pK_2) are very close to 5.2 [29], so it is at pH 7.0 in nonprotonated and at pH 4.0 in biprotonated form, respectively. The aim of this work was to study the effects of interaction of protonated and nonprotonated $TPPS_4$ with CTAB micelles on spectral (cross-sections) and dynamic (quantum yields and rate constants) characteristics of its ground and lowest singlet and triplet excited states.

3.1. Applied model

To analyze the experimental data we applied a five-level diagram (Fig. 1), which includes the molecule ground state singlet level (S_0), two excited singlet levels (S_1 and S_n) and two triplet levels (T_1 and T_m). Basing on the fact that in the spectral range, where $TPPS_4$ possesses absorption (resonant conditions), the excited state absorption (saturable absorption) prevails, as compared with simultaneous two-photon absorption (2PA) [30,31], we considered that observed nonlinear effects were due just to sequential absorption of two photons by ground and excited states and neglected any 2PA absorption. We have also considered that at room temperature the $TPPS_4$ molecule was in the lowest vibronic level of S_0 state and at excitation just the lowest vibronic levels of S_1 and T_1 states were populated, and the populations of higher vibronic and electronic excited states were negligible due to their short lifetimes as compared with the excitation pulse duration.

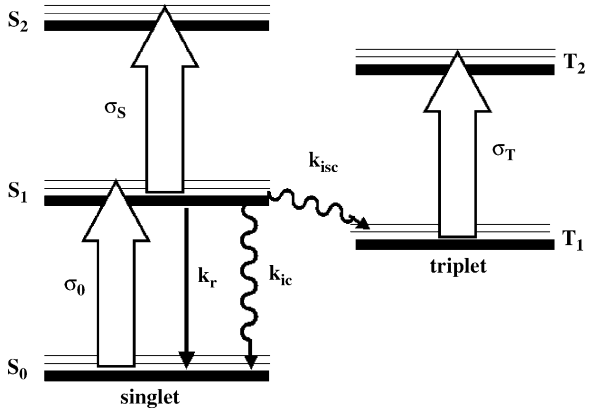

Fig. 1. Five-energy-level diagram.

3.2. Data obtained by linear optical methods

Using the linear methods we determined the values of the ground state cross-sections (σ_0) at $\lambda = 532$ nm, the fluorescence quantum yields Φ_{fl} and the lifetimes of S_1 (τ_S) and T_1 (τ_T) states of protonated and nonprotonated $TPPS_4$ in the presence and absence of CTAB micelles.

The σ_0 cross-section was determined directly from the solution linear absorbance at $\lambda = 532$ nm as

$$\sigma_0 = \frac{\alpha_0}{N} \tag{1}$$

where α_0 is the linear absorption and N is the $TPPS_4$ concentration.

The Φ_{fl} was determined by comparison with a standard, which was *meso*-tetrakis(4-*N*-methyl-pyridiniumyl) porphyrin (TMPyP) in its free base form in an aqueous solution at pH 6.8 ($\Phi_{fl0} = 0.05 \pm 0.01$) [32]. The Φ_{fl} was calculated according to the equation:

$$\Phi_{fl} = \Phi_{fl0} \frac{I_{fl}}{I_{fl0}} \frac{A_0}{A} \tag{2}$$

where Φ_{fl} is the $TPPS_4$ quantum yield, I_{fl} and I_{fl0} the integral fluorescence intensities of $TPPS_4$ and TMPyP in the spectral range from 600 to 800 nm induced by the excitation at $\lambda_{ex} = 580$ nm and A and A_0 are the absorbances of $TPPS_4$ and TMPyP at λ_{ex}, respectively.

The fluorescence decay curves (Fig. 2) were obtained using time-correlated single photon counting method at $\lambda_{ex} = 436$ nm and $\lambda_{em} = 672$ nm. The curve profiles were monoexponential for all the experimental conditions used. The lifetimes τ_S were calculated by single-exponential fitting these curves

$$I = I_0 \exp\left(\frac{-t}{\tau_S}\right) \tag{3}$$

The decay curves of the triplet–triplet absorption (Fig. 3) were obtained using a flash-photolysis technique of the deairated $TPPS_4$ solutions excited at $\lambda_{ex} = 355$ nm and registered at $\lambda = 470$ nm. Similarly to fluorescence the monoexponential

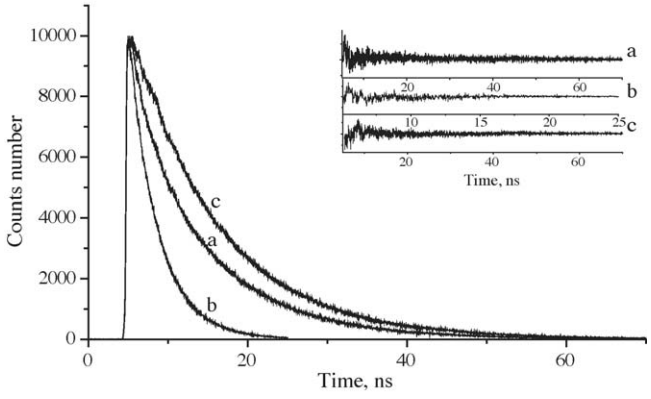

Fig. 2. Decay profiles of the fluorescence of $[TPPS_4] = 10$ μM monitored at 671 nm and excited at 532 nm in homogeneous solutions at pH 7.0 (a), at pH 4.0 (b) and in the presence of [CTAB] = 4.8 mM at pH 4.0 (c). *Insert:* Residuals of these decay profiles for single-exponential fits.

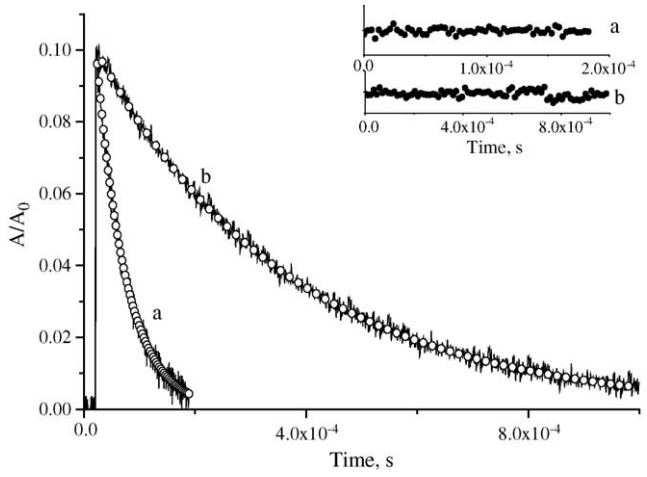

Fig. 3. Normalized decay profiles of the triplet state of [$TPPS_4$] = 10 μM monitored at 470 nm in deoxygenated solutions at pH 4.0 in the absence (a) and in the presence of [CTAB] = 4.8 mM (b); fitting of these profiles using single-exponential fits (◯ ◯ ◯). *Insert:* Residuals of these decay profiles for single-exponential fits.

profile of the triplet–triplet absorption decay was observed under all experimental conditions. This demonstrates that the contribution of bimolecular quenching processes between triplets, such as T–T annihilation, is low under conditions used. The lifetime τ_T were calculated by single-exponential fitting these curves

$$A = A_0 \exp\left(\frac{-t}{\tau_T}\right) \tag{4}$$

where A_0 and A are the solution absorbances directly after excitation and the current one, respectively.

3.3. Data obtained by nonlinear optical methods

Resonant nonlinear optical processes can be observed with sufficient reliability only at high irradiation levels, since their efficiency increases with the beam intensity. Consequently, to evaluate these photophysical parameters of the excited state it is necessary to employ especial techniques such as Z-scan and/or pulse train Z-scan.

In order to obtain cross-sections σ_S and σ_T, the triplet state quantum yield Φ_T and the internal conversion and intersystem crossing rate constants k_{ic} and k_{isc}, we used Z-scan techniques with single 70 ps pulse and with pulse trains (PTZ-scan).

During a single pulse or a pulse train the molecule can pass to S_n and/or T_m excited states. However, due to very short lifetimes of these states as compared with the pulse duration we have to assume that the S_n and T_m populations are negligible and just the populations of S_1 and T_1 states have to be taken into consideration.

A simplified three-level diagram can be applied to explain the single pulse effect. Indeed, the first state populated during the pulse action is S_1, with the lifetime τ_S, which depends on external conditions. For $TPPS_4$ τ_S is in the range from 3.6 to 11.0 ns. Since the 70 ps pulse duration is much shorter than this value, we can safely consider that the S_1 population of during the pulse is practically constant and the population of the triplet state is negligible. So in this case the normalized transmittance can be analyzed using just the left hand side of the diagram in Fig. 1. Consequently, the rate equation used to describe the fraction of molecules at the ground state is:

$$\frac{dn_{S_0}}{dt} = -W_{S_0 \to S_1} n_{S_0} \tag{5}$$

where $W_{S_0 \to S_1} = \frac{\sigma_0 I}{h\nu}$ is the upward one-photon transition rate and n_{S_0} is the population fraction of the ground state. Since the population of the excited states S_n was neglected,

$$n_{S_0} + n_{S_1} = 1 \tag{6}$$

where n_{S_1} is the population fraction of the first excited singlet state S_1. Eq. (5) can be easily integrated using the initial condition $n_{S_0}(-\infty) = 1$, resulting in:

$$n_{S_0}(t) = \exp\left\{-\frac{\sigma_0 F(t)}{h\nu}\right\} \tag{7}$$

where $F(t) = \int_{-\infty}^{t} I(t)dt$ is the fluence incidence on the sample from $-\infty$ to t.

For this type of systems the time-dependence of the absorption coefficient during the excitation pulse is given by:

$$\alpha(t) = N[n_{S_0}(t)\sigma_0 + n_{S_1}(t)\sigma_S] = \alpha_0\left[1 + n_{S_1}(t)\left(\frac{\sigma_S}{\sigma_0} - 1\right)\right] \tag{8}$$

where σ_S is the absorption cross-section of the excited singlet state and $n_{S_0} = 1 - n_{S_1}$. The Beer's law equation governing the variation of the irradiance, I, along the penetration depth, z, can be written as:

$$\frac{dI}{dz} = -\alpha(t)I(t) = -\alpha_0\left\{1 + \left(\frac{\sigma_S}{\sigma_0} - 1\right)\left(1 - \exp\left\{\frac{\sigma_0 F(t)}{h\nu}\right\}\right)\right\} I(t) \tag{9}$$

Since in our Z-scan experiments the detection system measures the pulse fluence, we integrate numerically this equation over the full pulse width (over t from $-\infty$ to $+\infty$) and over the sample thickness. The result is then normalized to the linearly transmitted energy, $\varepsilon = \varepsilon_0 \exp\{-\alpha_0 L\}$, and used to fit the data in Fig. 4, as shown by the solid lines. This procedure gives the only adjustable parameter σ_S.

Since the duration of Q-switch envelope is about 200 ns and the time interval between consecutive pulses is 13 ns, there is enough time to depopulate the S_1 state and the part of the excited molecules pass to T_1 due to intersystem crossing process. Thus PTZ-scan measurements present an accumulative nonlinearity due to the population of the long-lived triplet state and it is necessary to apply the diagram (Fig. 1) in its complete form. We assume that the T_1 lifetime is too long, as compared with the pulse train duration, so in this case the depopulation of the T_1 state can be ignored. Considering the relaxation from the S_1 state, the rate equations used to describe the fractions of

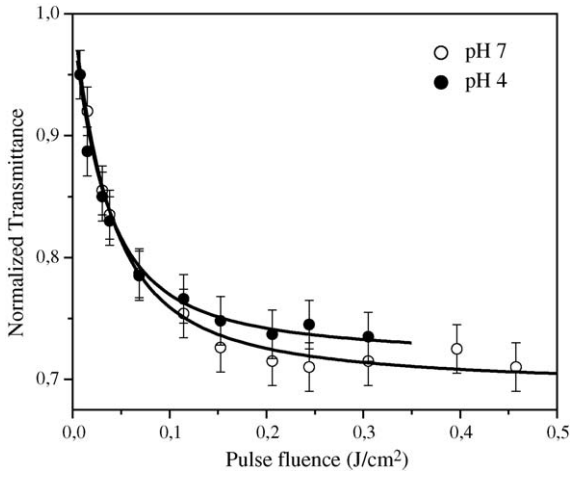

Fig. 4. Normalized transmittance for the $TPPS_4$ in the presence of CTAB as a function of the pulse fluence. The molecules number used were 7×10^{16} and 5×10^{16}, for pH 7 and 4, respectively. Solid lines are fittings obtained with the procedure described in the text.

molecules in each level are given by:

$$\frac{dn_{S_0}}{dt} = -W_{S_0 \to S_1} n_{S_0} + n_{S_1}\left(\frac{1}{\tau_f} - k_{isc}\right) \quad (10)$$

$$\frac{dn_{S_1}}{dt} = W_{S_0 \to S_1} n_{S_0} - \frac{n_{S_1}}{\tau_f} \quad (11)$$

$$\frac{dn_{T_1}}{dt} = n_{S_1} k_{isc} \quad (12)$$

We also have the normalization condition $n_{S_0} + n_{S_1} + n_{T_1} = 1$. When a 70 ps mode-locked pulse is present, Eqs. (10)–(12) are solved, producing new values for the population. Between pulses, the sample appears in the dark ($W_{S_0 \to S_1} = 0$) and only relaxation terms are considered. In this way, the populations can be mapped along the complete Q-switch envelope provided that the temporal intensity pattern of the pulse train are actually employed in the experiment and the initial conditions $n_{S_0}(-\infty) = 1$, $n_{S_1}(-\infty) = n_{T_1}(-\infty) = 0$ are met. This procedure yields the population time evolution necessary to determine the excited states parameters. Taking into account the triplet manifold of Fig. 5, as well, the transmittance evolution is found as given by the equation below:

$$\frac{dI}{dz} = -N[n_{S_0}\sigma_0 + n_{S_1}\sigma_S + n_{T_1}\sigma_T] \quad (13)$$

The values of the intersystem crossing time and triplet excited state absorption cross-section were obtained by the best PTZ-scan data fitting, by numerically solving Eqs. (10)–(13) and normalization of the result by linearly transmitted energy. The PTZ-scan data and theoretical adjusts are depicted in Fig. 5.

Finally, the σ_0, σ_S, σ_T, τ_T, Φ_{fl}, Φ_T and k_{isc} values were obtained from the experiment. The rate constant k_r was calculated from Eqs. (2) and (3) as

$$k_r = k_{isc}\frac{\Phi_{fl}}{\Phi_T} \quad (14)$$

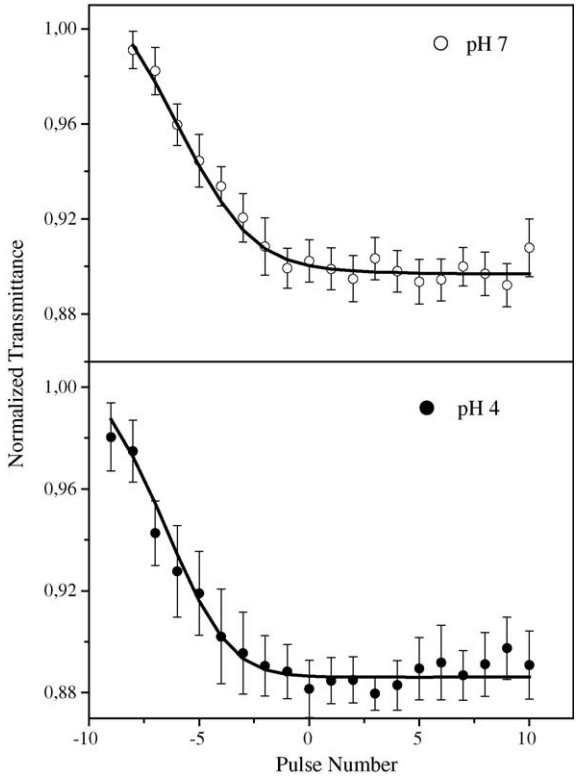

Fig. 5. Pulse train Z-scan measurements for $TPPS_4$ in the presence of CTAB. The strongest pulse of the train was labeled '0'.

Taking into account that

$$\frac{1}{\tau_{fl}} = k_r + k_{ic} + k_{isc} \quad (15)$$

we obtained k_{ic} as

$$k_{ic} = \frac{1}{\tau_{fl}} - k_r - k_{isc} \quad (16)$$

The interconversion quantum yield was calculated as

$$\Phi_{ic} = 1 - (\Phi_{fl} + \Phi_T) \quad (17)$$

All the characteristics are listed in Table 1. Some of them have already been determined formerly [18–22] and our results are in accordance with them.

The comparison of the obtained values at pH 7.0 and 4.0 demonstrates that protonation strongly affects all studied characteristics. So, at $\lambda = 532$ nm protonation reduces σ_0 and increases σ_S and σ_T. It reduces τ_S, as well, inducing the ≅2-fold increase of k_r, as well as a slight increase of k_{isc} and the dramatic one of k_{ic}, which makes the internal conversion dominant for protonated $TPPS_4$. The increase of k_r induces the slight increase of Φ_{fl}. The Φ_T suffers the two-fold reduction. This reduction should be explained by the increase of k_r and, especially, of k_{ic}, which compensate the k_{isc}. The increase of k_{isc} agrees with the reduction of τ_T, both demonstrating the increase of the probability of the intersystem crossing at protonation.

The values of all the characteristics in the presence of CTAB micelles at both pHs are close to those at pH 7.0 in homogeneous solutions and quite different from those at pH 4.0. This result is in

Table 1
Cross-sections values for the ground (σ_0), excited singlet (σ_S) and excited triplet (σ_T) states at $\lambda = 532$ nm, S_1 and T_1 state lifetimes (τ_S and τ_T), fluorescence (Φ_{fl}), triplet (Φ_T) and internal conversion (Φ_{ic}) quantum yields and the rates constants of intersystem crossing (k_{isc}), radiative (k_r) and internal conversion (k_{ic}) of protonated and nonprotonated $TPPS_4$ in the presence and in the absence of CTAB micelles

pH	[CTAB] (mM)	σ_0 (10^{-17} cm^2)	σ_S (10^{-17} cm^2)	σ_T (10^{-17} cm^2)	τ_S (ns)	τ_T (μs)	Φ_{fl}	Φ_T	Φ_{ic}	k_{isc} (10^8 s^{-1})	k_r (10^8 s^{-1})	k_{ic} (10^8 s^{-1})
4.0	0	0.8	7.4	7.6	3.6	54	0.37	0.36	0.37	1.0	1.0	0.75
4.0	4.8	1.9	4.8	2.9	11.0	350	0.14	0.79	0.07	0.71	0.13	0.07
7.0	0	2.1	4.7	3.3	9.0	360	0.16	0.77	0.07	0.77	0.16	0.07
7.0	4.8	1.9	4.8	2.9	11.0	350	0.14	0.79	0.07	0.71	0.13	0.07

accordance with the observation that the interaction with CTAB micelles shifts the pK_a point of $TPPS_4$ from 5.0 to 2.5 and at pH 4.0 $TPPS_4$ bound with micelle appears in its nonprotonated state [16]. Moreover, we can conclude that for the nonprotonated $TPPS_4$ the change of the environment from homogeneous aqueous solution to the micellar one affects weakly its characteristics.

The reduction of the sample transmittance, named the reverse saturable absorption (RSA), was observed at both pHs in both regimes, single pulse and PTZ-scan. This effect appears because for all regimes the cross-sections of the excited state σ_S and σ_T are larger than that of ground state σ_0. Indeed, the difference between the absorbance of the sample under irradiation (α_{irr}) and the initial one (α_{in}) is

$$\Delta\alpha = \alpha_{irr} - \alpha_{in} = (\sigma_{ex} - \sigma_0)N_{ex} \quad (18)$$

where σ_{ex} is the excited state cross-section (σ_S or σ_T) and N_{ex} is the concentration of excited molecules. Thus, for the same of an excited state population the larger is the difference ($\sigma_{ex} - \sigma_0$), the larger is $\Delta\alpha$. So, the effect is larger for the protonated $TPPS_4$. At the same time, for the nonprotonated $TPPS_4$, both in the presence and in the absence of CTAB, the RSA is more pronounced for the single pulse regime, as the difference $\sigma_S - \sigma_0$ is larger than $\sigma_T - \sigma_0$.

The efficiency of a limiter increases when increases the $\Delta\alpha$. This means that $TPPS_4$ in its nonprotonated form is expected to be more effective as a fast optical limiter or a fast switcher in the femto- or picosecond time range that in the nanosecond one.

Binding with micelles does not change practically either Φ_T or τ_T of the nonprotonated $TPPS_4$. The same result has already been observed at its binding with bovine serum albumin [14] and *ghost* cells [Aggarwal, Gonçalves, Ciancaglini, Borissevitch, in preparation]. Thus, it is reasonable to expect, that the $TPPS_4$ binding with the microstructures in the organism should not affect strongly these characteristics, as well. However, this does not mean that its efficacy in PDT would suffer no changes, for example, due to reduced probability of the $TPPS_4$ triplet quenching by molecular oxygen [Aggarwal, Gonçalves, Borissevitch, in preparation], which could reduce the singlet oxygen formation.

Acknowledgments

We gratefully acknowledge the support of Fundação de Amparo à Pesquisa do Estado de São Paulo (FAPESP), Conselho Nacional de Desenvolvimento Científico e Tecnológico (CNPq) and Coordenação de Aperfeiçoamento de Pessoal de Nível Superior (CAPES).

References

[1] M. Calvete, G.Y. Yang, M. Hanack, Synth. Met. 141 (2004) 231–243.
[2] C.P. Singh, K.S. Bindra, B. Jain, S.M. Oak, Opt. Commun. 245 (2005) 407–414.
[3] K. Kandasamy, K.D. Rao, R. Deshpande, P.N. Puntambekar, B.P. Singh, S.J. Shetty, T.S. Srivastava, Appl. Phys. B 64 (1997) 479–484.
[4] R. Bonnett, Chem. Soc. Rev. 24 (1995) 19–33.
[5] M. Ochsner, J. Photochem. Photobiol. 39 (1997) 1–18.
[6] E. Ben-Hur, B. Horowitz, Photochem. Photobiol. 62 (1995) 383–388.
[7] D.E. Lewis, R.E. Utecht, M.M. Judy, L.J. Matthews, T.C. Chanh, Spectrum 6 (1993) 8–10.
[8] J.B. Cannon, J. Pharm. Res. 82 (1993) 435–446 (and references therein).
[9] J.W. Winkelman, Cancer Res. 22 (1962) 589–596.
[10] P. Engst, P. Kubát, M. Jirsa, J. Phochem. Photobiol. A: Chem. 78 (1994) 215–219.
[11] I. Borissevitch, N.N. Rakov, G.S. Maciel, C.B. de Araújo, Appl. Opt. 39 (2000) 4431–4435.
[12] P.J. Goncalves, L. De Boni, N.M.B. Neto, J.J. Rodrigues, S.C. Zilio, I.E. Borissevitech, Chem. Phys. Lett. 407 (2005) 236–241.
[13] K. Lang, J. Mosinger, D.M. Wagnerova, Coord. Chem. Rev. 248 (2004) 321–350.
[14] I. Borissevitch, T.T. Tominaga, H. Imasato, M. Tabak, J. Lumin. 69 (1996) 65–76.
[15] I. Borissevitch, T.T. Tominaga, C.C. Schmitt, J. Photochem. Photobiol. A: Chem. 114 (1998) 201–207.
[16] S.C.M. Gandini, V.E. Yushmanov, I.E. Borissevitch, M. Tabak, Langmuir 15 (1999) 6233–6243.
[17] I.E. Borissevitch, C.P.F. Borges, G.P. Borissevitch, V.E. Yushmanov, S.R.W. Louro, M. Tabak, Z. Naturforsc. [C] J. Biosci. 51/7–8 (1996) 578–590 (and references therein).
[18] R. Bonnet, R.J. Ridge, E.J. Land, R.S. Sinclair, D. Tait, T.G. Truscott, J. Chem. Soc., Faraday Trans. I 78 (1982) 127–136.
[19] K. Kalyanasundaram, Photochemistry of Polypyridine and Porphyrin Complexes, Academic Press, New York, 1991, p. 420.
[20] D.L. Akins, S. Ozcelik, H.R. Zhu, C. Guo, J. Phys. Chem. 100 (1996) 14390–14396.
[21] P. Kubat, J. Mosinger, J. Photochem. Photobiol. A: Chem. 96 (1996) 93–97.
[22] N.C. Maiti, S. Mazumdar, N. Periasamy, J. Phys. Chem. B 102 (1998) 1528–1538.
[23] M. Sheik-Bahae, A.A. Said, E.W. Van Stryland, Opt. Lett. 14 (1989) 955–957.
[24] M. Sheik-Bahae, A.A. Said, T. Wei, D.J. Hagan, E.W. Van Stryland, IEEE J. Quant. Electron. 26 (1990) 760–769.
[25] T.H. Wei, T.H. Huang, T.C. Wen, Chem. Phys. Lett. 314 (1999) 403–410.
[26] T.H. Wei, T.H. Huang, T.T. Wu, P.C. Tsai, M.S. Lin, Chem. Phys. Lett. 318 (2000) 53–57.

[27] Z. Sun, M. Tong, H. Zeng, L. Ding, Z. Wang, J. Opt. Soc. Am. B 18 (2001) 1464–1468.
[28] L. Misoguti, C.R. Mendonca, S.C. Zilio, Appl. Phys. Lett. 74 (1999) 1531–1533.
[29] V.E. Yushmanov, H. Imasato, T.T. Tominaga, M. Tabak, J. Inorg. Biochem. 61 (1996) 233–241.
[30] A.A. Andrade, N.M. Barbosa Neto, L. Misoguti, L. De Boni, S.C. Zilio, C.R. Mendonça, Chem. Phys. Lett. 390 (2004) 506–510.
[31] L. De Boni, A.A. Andrade, D.S. Corrêa, D.T. Balogh, S.C. Zilio, L. Misoguti, C.R. Mendonça, J. Phys. Chem. B 108 (2004) 5221–5224.
[32] V.M. de Paoli, S.H. de Paoli, I.E. Borissevitch, A.C. Tedesco, J. Alloys Compd. 344 (2002) 27–31.